

# Spatial soliton switching in quasi-continuous optical arrays

Yaroslav V. Kartashov,\* Anna S. Zelenina,\* and Lluís Torner

ICFO–Institut de Ciències Fòniques and Department of Signal Theory and Communications,  
Universitat Politècnica de Catalunya, 08034 Barcelona, Spain

Victor A. Vysloukh

Departamento de Física y Matemáticas, Universidad de las Américas—Puebla,  
Santa Catarina Martir, CP 72820, Puebla, Cholula, Mexico

Received October 7, 2003

We report on the phenomenon of trapping and switching of one-dimensional spatial solitons in Kerr-type nonlinear media with transverse periodic modulation of the refractive index. The solitons slowly radiate upon propagation along the periodic structure and are finally trapped in one of its guiding channels. The position of the output channel can be varied by small changes in the launching angle. © 2004 Optical Society of America

OCIS codes: 190.5530, 190.4360, 060.1810.

The propagation of light in media whose properties vary periodically along the transverse direction exhibits a wealth of opportunities for all-optical control of light. A key parameter is the competition between characteristic scales of the problem, namely, the beam width and transverse modulation period. For localized excitations in evanescently coupled waveguides, such competition leads to the formation of discrete solitons.<sup>1,2</sup> Discrete solitons have been observed experimentally<sup>3</sup> and have been suggested to be useful for a number of potential practical applications, including all-optical soliton steering and switching.<sup>2–11</sup> However, the intermediate regime constituted by continuous nonlinear media with an imprinted transverse modulation of the refractive index offers a variety of new opportunities.<sup>12,13</sup> The concept behind such potential might be termed tunable discreteness, with the strength of modulation being the parameter that tunes the system properties from continuous to discrete. In this context, spatial optical solitons have recently been experimentally demonstrated in arrays of optically induced waveguides.<sup>14–16</sup> Such light-induced structures might operate in both weakly and strongly coupled regimes between neighboring guides, thus offering the above-mentioned tunability. In this Letter we consider soliton propagation in Kerr nonlinear media with harmonic modulation of the refractive index and show that radiative coupling can lead to controllable trapping of light in the different locations of the array, an effect that allows interpolation within the different steering properties of continuous and discrete solitons.

The propagation of radiation along the  $z$  axis in a slab waveguide with periodic modulation of the linear refractive index in the  $x$  direction and focusing the Kerr-type nonlinearity is described by the nonlinear Schrödinger equation

$$i \frac{\partial q}{\partial \xi} = -\frac{1}{2} \frac{\partial^2 q}{\partial \eta^2} - q|q|^2 - pR(\eta)q. \quad (1)$$

Here  $q(\eta, \xi) = (L_{\text{dif}}/L_{\text{nl}})^{1/2} A(\eta, \xi) I_0^{-1/2}$ , where  $A(\eta, \xi)$  is the slowly varying envelope,  $I_0$  is the input inten-

sity,  $\eta = x/r_0$ ,  $r_0$  is the input beam width,  $\xi = z/L_{\text{dif}}$ ,  $L_{\text{dif}} = n_0 \omega r_0^2/c$ ,  $L_{\text{nl}} = 2c/\omega n_2 I_0$ ,  $\omega$  is the frequency,  $p = L_{\text{dif}}/L_{\text{ref}}$  is the guiding parameter,  $L_{\text{ref}} = c/(\delta n \omega)$ ,  $\delta n$  is the refractive index modulation depth,  $R(\eta) = \cos(2\pi\eta/T)$  describes the refractive-index profile, and  $T$  is the modulation period. We assume that the depth of the refractive-index modulation is small compared with the unperturbed index  $n_0$  and is of the order of the nonlinear correction to the refractive index because of the Kerr effect. Equation (1) admits several conserved quantities, including the energy flow  $U = \int_{-\infty}^{\infty} |q|^2 d\eta$ .

The regimes of beam propagation in the periodic grating [Eq. (1)] can be classified with the aid of the simple effective-particle approach. This approach is based on the following equations:

$$\begin{aligned} \frac{d^2}{d\xi^2} \langle \eta \rangle &= \frac{p}{U} \int_{-\infty}^{\infty} |q|^2 \frac{dR}{d\eta} d\eta, \\ \frac{d^2}{d\xi^2} \langle (\eta - \langle \eta \rangle)^2 \rangle &= \frac{2}{U} \int_{-\infty}^{\infty} \left[ \left| \frac{\partial q}{\partial \eta} \right|^2 \right. \\ &\quad \left. + p|q|^2 \frac{dR}{d\eta} (\eta - \langle \eta \rangle) - \frac{1}{2} |q|^4 \right] d\eta \\ &\quad + \frac{2}{U^2} \left( \int_{-\infty}^{\infty} \frac{\partial q}{\partial \eta} q^* d\eta \right)^2 \end{aligned} \quad (2)$$

for quantities  $\langle \eta \rangle = (1/U) \int_{-\infty}^{\infty} |q|^2 \eta d\eta$  and  $\langle (\eta - \langle \eta \rangle)^2 \rangle = (1/U) \int_{-\infty}^{\infty} |q|^2 (\eta - \langle \eta \rangle)^2 d\eta$  that describe the evolution of the integral beam center and a mean square of the beam width. The approach requires substitution of  $q(\eta, \xi)$  into the right-hand parts of Eqs. (2), where one assumes that the beam shape remains unchanged upon propagation in the periodic grating. We chose  $q(\eta, \xi) = q_0 \text{sech}[\chi(\eta - \langle \eta \rangle)] \times \exp[i\alpha(\eta - \langle \eta \rangle) + i\phi]$ , where  $q_0$  is the beam amplitude,  $\chi$  is the form factor or inverse beam width,  $\alpha$  is the incident angle, and  $\phi$  is the phase. This choice of trial function is justified since, in the limit  $p \rightarrow 0$ , it describes soliton beams at  $q_0 = \chi$ . Substitution of

$q(\eta, \xi)$  and  $R(\eta)$  into Eq. (2) yields

$$\begin{aligned} \frac{d^2}{d\xi^2} \langle \eta \rangle &= -\frac{2\pi p}{T} \frac{\pi^2/T\chi}{\sinh(\pi^2/T\chi)} \sin\left(\frac{2\pi\langle \eta \rangle}{T}\right), \\ \frac{d^2}{d\xi^2} \langle (\eta - \langle \eta \rangle)^2 \rangle &= \frac{2}{3} (\chi^2 - q_0^2) - 2p \frac{\pi^2/T\chi}{\sinh(\pi^2/T\chi)} \\ &\quad \times \left[ \frac{\pi^2/T\chi}{\tanh(\pi^2/T\chi)} - 1 \right] \cos\left(\frac{2\pi\langle \eta \rangle}{T}\right). \end{aligned} \quad (3)$$

Let the beam be launched into the medium at the point  $\eta = 0$ , so that  $\langle \eta \rangle_{\xi=0} = 0$  and  $(d\langle \eta \rangle/d\xi)_{\xi=0} = \alpha$ . It follows from Eqs. (3) that a soliton can be considered as an effective particle moving in harmonic potential, whereas the integral beam center is equivalent to the particle position. Growth of the incident angle  $\alpha$  corresponds to an increase in the kinetic energy of the equivalent particle. At small kinetic energies the particle remains located in the central potential well (i.e., the light beam oscillates around the central waveguide). When the initial kinetic energy is larger than the height of the potential barrier, the particle leaves the central well and starts to travel along the structure. This critical value of the incident angle separating both regimes is given by  $\alpha_{cr} = 2[p(\pi^2/T\chi)\sinh^{-1}(\pi^2/T\chi)]^{1/2}$ . Trajectories of the beam center are described by  $\langle \eta \rangle = (T/\pi)\arcsin[m\text{sn}(\pi\alpha_{cr}\xi/T, m)]$  for  $\alpha < \alpha_{cr}$  ( $m = \alpha/\alpha_{cr}$ ) and by  $\langle \eta \rangle = (T/\pi)\arcsin[\text{sn}(\pi\alpha\xi/T, m)]$  for  $\alpha > \alpha_{cr}$  ( $m = \alpha_{cr}/\alpha$ ). The second of Eqs. (3) allows the amplitude  $q_0$  of stationary guided waves to be obtained under the assumption that the mean-square width remains unchanged upon propagation. In the limit of a narrow beam ( $\chi T \gg 1$ ), as well as for a wide beam ( $\chi T \ll 1$ ), the second of Eqs. (3) predicts that the mean-square width will remain constant for all values of  $\langle \eta \rangle$  if  $q_0 = \chi$ .

Results of the analytical treatment are confirmed by numerical simulations. We solved Eq. (1) with the split-step Fourier method for  $q(\eta, \xi = 0) = \chi \text{sech}(\chi\eta)\exp(i\alpha\eta)$ . The propagation of the beam along the periodic grating at  $\alpha > \alpha_{cr}$  is illustrated in Fig. 1(a). In this case the input beam width is comparable with the modulation period, whereas the incident angle is far above the critical angle. Figure 1(b) illustrates oscillations of the narrow beam in the central waveguide of the grating with a large period for  $\alpha < \alpha_{cr}$ . Analytical dependencies of the critical angle and the amplitude of the stationary guided wave on the period  $T$  calculated from Eqs. (3) at  $\langle \eta \rangle \equiv 0$  are shown in Figs. 2(a) and 2(b). The fast growth of  $\alpha_{cr}$  with increasing  $T$  is followed by saturation. The narrower the input beam, the higher the critical angle and the smaller the deviation of  $q_0$  from  $\chi$ . The guided-wave amplitude is always smaller than that for the soliton beam in a uniform medium and approaches  $\chi$  as guiding parameter  $p \rightarrow 0$ .

Numerical simulations indicate that beams moving along the grating slowly radiate—an effect not captured by the effective-particle approach. When soli-

tons cross the waveguide, they lose a fraction of their energy because the wing of the soliton spatial spectrum overlaps the spatial spectrum of the guided mode. The radiation rate increases as the incident angle approaches angle  $\alpha_b$ , corresponding to the edge of the first Brillouin zone.<sup>12,13</sup> The energy losses caused by the excitation of consecutive waveguides result in the slant soliton beam being trapped in one of the grating channels. This situation is shown in Fig. 1(c). Note that the propagation distance at which trapping occurs is relatively small. Intuitively, it is clear that the larger the incident angle, the higher the channel number at which trapping occurs. Such radiative trapping has much in common with the properties of discrete solitons in waveguide arrays; the main

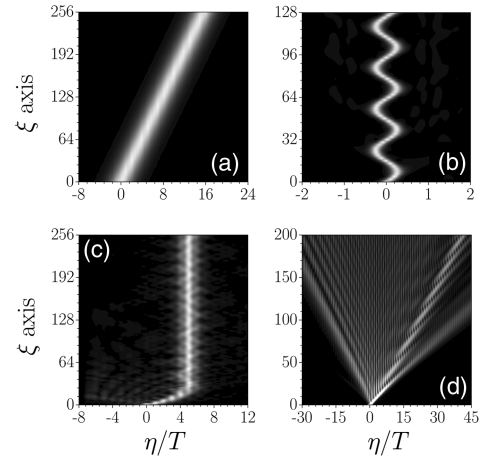


Fig. 1. Different regimes of soliton propagation in the medium with harmonic modulation of the linear refractive index: (a) Undistorted propagation at  $T = \pi/4$ ,  $p = 1$ ,  $\alpha = 0.05$ . (b) Oscillations within the central channel at  $T = 4\pi$ ,  $p = 0.25$ ,  $\alpha = 0.7$ . (c) Fast switching to the fifth channel at  $T = \pi/2$ ,  $p = 1$ ,  $\alpha = 0.8$ . (d) Radiative decay at  $T = \pi$ ,  $p = 0.25$ ,  $\alpha = 1.13$ .

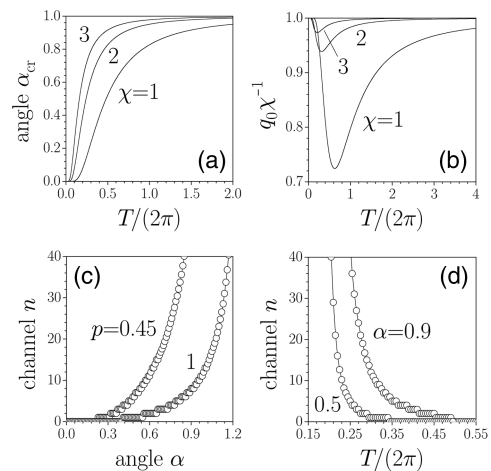


Fig. 2. (a) Critical angle and (b) amplitude of a stationary guided wave versus period of the refractive-index modulation at  $p = 0.25$  for various values of form factor  $\chi$ . (c) Dependence of the number of the output channel on the incident angle at  $T = \pi/2$  for different guiding parameters. (d) Dependence of the number of the output channel on the period of the refractive-index modulation at  $p = 0.5$  for different incident angles.

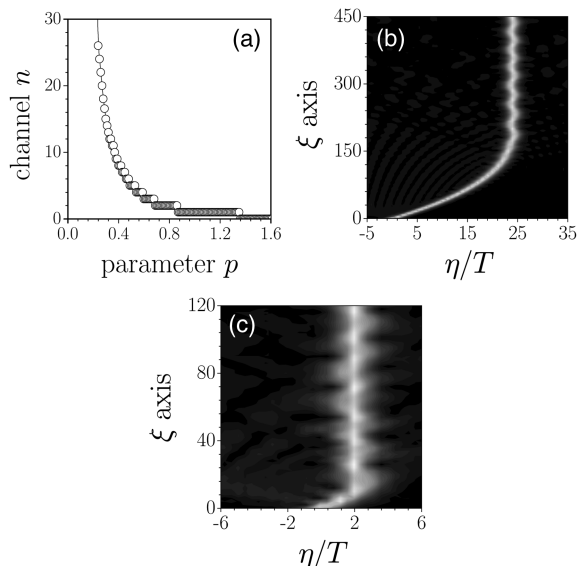


Fig. 3. (a) Dependence of the number of the output channel on the guiding parameter at  $T = \pi/2$  and  $\alpha = 0.5$ . (b) and (c) Modification of spatial soliton mobility for  $p = 0.25$  and  $p = 0.7$ , respectively.

difference is that in the strong-coupling model analyzed here the moving soliton is a quasi-continuous entity. Figure 2(c) shows the dependence of the number of the output channel versus the incident angle. We assume that the soliton is trapped in the  $n$ th channel if  $nT - T/2 \leq \langle \eta \rangle \leq nT + T/2$  when  $\xi \rightarrow \infty$ . The width of the interval of angles corresponding to trapping in the fixed channel decreases with increasing channel number. At high angles the small growth of the incident angle results in a considerable increase in the channel number. The smaller the guiding parameter, the sharper the switching curve. Switching can be effectively realized in limited intervals of incident angles  $0 < \alpha < \alpha_b$ , since at  $\alpha \approx \alpha_b$  the input beam is completely disintegrated because of the Bragg reflection from the periodic structure [see Fig. 1(d)]. Note that  $\alpha_b \rightarrow \infty$  as modulation period  $T \rightarrow 0$ .

Because beams radiate upon motion along the grating, the energy flow in the output channel drops with increasing channel number. In typical situations such as the one depicted in Fig. 1(c), the energy losses are of the order of 25% of the input value even for outputs located at the 50th channel. The energy radiation rate decreases with a decrease in the modulation period. Already at  $T = \pi/4$  (which is of the same order as the soliton width) the soliton is barely affected by the periodic variation of the refractive index and thus propagates as in a uniform medium even for considerable depth of refractive-index modulation  $p = 1$  [Fig. 1(a)]. Figure 2(d) shows the dependence of the output channel on the period of the modulation at a fixed incident angle. Note the rapid growth of the radiation loss rate that is accompanied by a decrease in the number of the output channel. The output channel number decreases with increasing guiding parameter. Such behavior, which supports the central idea

of tunable discreteness put forward here, is illustrated in Fig. 3. Figures 3(a) and 3(b) demonstrate the possibility of controlling the soliton mobility by varying the refractive-index modulation depth, i.e., the effective discreteness of the lattice.

To conclude, we stress that we have addressed the intermediate regime between fully continuous and fully discrete behavior of solitons propagating in nonlinear media with imprinted periodic refractive-index modulations and have shown that it offers a variety of new opportunities for the all-optical manipulation of light signals. The new control parameter is the depth, or the period, of the modulation. The concept could be implemented in practice in optically induced periodic guiding structures.<sup>14–18</sup>

This work was partially supported by the Generalitat de Catalunya and by the Spanish Government through grant TIC2000-1010. Y. Kartashov's e-mail addresses are azesh@genphys.phys.msu.ru and yaroslav.kartashov@upc.es.

\*Also with the Department of Physics, M. V. Lomonosov Moscow State University, 119899 Vorobiovy Gory, Moscow, Russia.

## References

1. D. N. Christodoulides and R. I. Joseph, *Opt. Lett.* **13**, 794 (1988).
2. D. N. Christodoulides, F. Lederer, and Y. Silberberg, *Nature* **424**, 817 (2003).
3. H. S. Eisenberg, Y. Silberberg, R. Morandotti, A. R. Boyd, and J. S. Aitchison, *Phys. Rev. Lett.* **81**, 3383 (1998).
4. W. Krolikowski, U. Trutschel, M. Cronin-Golomb, and S. Schmidt-Hattenberger, *Opt. Lett.* **19**, 320 (1994).
5. R. Muschall, C. Schmidt-Hattenberger, and F. Lederer, *Opt. Lett.* **19**, 323 (1994).
6. A. B. Aceves, C. De Angelis, S. Trillo, and S. Wabnitz, *Opt. Lett.* **19**, 332 (1994).
7. W. Krolikowski and Y. S. Kivshar, *J. Opt. Soc. Am. B* **13**, 876 (1996).
8. O. Bang and P. D. Miller, *Opt. Lett.* **21**, 1105 (1996).
9. T. Pertsch, U. Peschel, and F. Lederer, *Opt. Lett.* **28**, 102 (2003).
10. D. N. Christodoulides and E. D. Eugenieva, *Phys. Rev. Lett.* **87**, 233901 (2001).
11. D. N. Christodoulides and E. D. Eugenieva, *Opt. Lett.* **26**, 1876 (2001).
12. R. Scharf and A. R. Bishop, *Phys. Rev. E* **47**, 1375 (1992).
13. O. Cohen, T. Schwartz, J. W. Fleischer, M. Segev, and D. N. Christodoulides, *Phys. Rev. Lett.* **91**, 113901 (2003).
14. N. K. Efremidis, S. Sears, D. N. Christodoulides, J. W. Fleischer, and M. Segev, *Phys. Rev. E* **66**, 046602 (2002).
15. J. W. Fleischer, M. Segev, N. K. Efremidis, and D. N. Christodoulides, *Nature* **422**, 147 (2003).
16. D. Neshev, E. Ostrovskaya, Y. Kivshar, and W. Krolikowski, *Opt. Lett.* **28**, 710 (2003).
17. P. J. Y. Louis, E. A. Ostrovskaya, C. M. Savage, and Y. S. Kivshar, *Phys. Rev. A* **67**, 013602 (2003).
18. N. K. Efremidis and D. N. Christodoulides, *Phys. Rev. A* **67**, 063608 (2003).